Algorithms Theoretical Basis Document for OSI SAF MTG radiative fluxes

Products OSI–303-b, OSI-304-b

Version : 0.2

Date : 04/05/2017

Prepared by Anne Marsouin, Météo-France/CMS

Document Change record

Document version	Software version	Date	Author	Change description
0.1		28/03/2017	AM	First version submitted to EUMETSAT
0.2		04/05/2017	AM	Updated version taking into accounts RIDs from the PDCR (Preliminary system architecture Design and Component consolidation design Review) 1.3: two references added in response to rid 25 1.5: applications and requirements summarized in response to rids 25 and 42 4.1: definition of MTG products recalled in response to rid 47 4.2: changing MTG slots used in hourly products in response to rid 47 6.2: validation before operations is mentioned in response to rid 25 6.2.1: MDS files contain SDI, in response to rid 52 6.2.2: figure 5 added in response to rid 43

Contents

1. Introduction

1.1. Scope of the document

The EUMETSAT Satellite Application Facilities (SAFs) are dedicated centres of excellence for processing satellite data. They form an integral part of the distributed EUMETSAT Application Ground Segment. The Ocean and Sea Ice SAF, led by Météo-France/Centre de Météorologie Spatiale (M-F/CMS), has the responsibility of developing, validating and distributing products of Radiative Fluxes derived from imagers on board GEO or LEO satellites. Such products are presently derived from MSG and GOES-E imagers. More information can be found at http://www.osi-saf.org.

This document is written in the framework of the PDCR (Preliminary and Design Component Consolidation Review) and concerns the radiative fluxes derived from the Flexible Combined Imager (FCI) on MTG satellites. It describes the algorithms and the main features of the processing.

1.2. Definitions and acronyms

The Surface Solar Irradiance (SSI) is the solar irradiance reaching the Earth surface in the 0.3-4 µm band, the irradiance being the radiant flux received per unit area.

The Downward Longwave Irradiance (DLI) is the irradiance reaching the Earth surface in the 4-100 µm band.

BDRF	bi-directional reflectance function
CERES	Clouds and Earth's Radiant Energy System
CMS	Centre de Météorologie Spatiale
CM SAF	Climate SAF
DLI	Downward Longwave Irradiance
ECMWF	European Center for Medium range Weather Forecast
GOES	Geostationary Operational Environmental Satellite
GOES-E	GOES East
FCI	Flexible Combined Imager
FDC	Full Disk Coverage
LML	Low and Mid Latitudes
LSA SAF	Land Surface Analysis SAF
MDS	Match up Data Set
NWC SAF	Nowcasting and very short range forecasting SAF
OSI SAF	Ocean and Sea Ice SAF
PDCR	Preliminary and Design Component Consolidation Review
RTM	Radiative Transfer Model
SAF	Satellite Application Facility
SDI	Saharan Dust Index
SEVIRI	Spinning Enhanced Visible and Infrared Imager
SSI	Surface Solar Irradiance
SST	Sea Surface Temperature
TOA	Top of atmosphere
UT	Universal Time

1.3. Reference documents

[RD.1] NWC SAFF, Algorithm Theoretical Basis Document for the Cloud Product Processors of the NWC/GEO MTG-I day-1, version 10d, 09/01/2017
NWC/CDOP2/MTG/MFL/SCI/ATBD/Cloud

[RD.2] METEOSAT and GOES-E Radiative Fluxes Validation Report (products OSI-303, 304, 305, 306) Version 1.2 June 2011.
SAF/OSI/CDOP/M-F/TEC/MA/184

[RD.3] OSI SAF CDOP2 HALF-YEARLY OPERATIONS REPORT, 2nd half 2016.
SAF/OSI/CDOP2/M-F/TEC/RP/338

1.4. Applicable documents

[AD.1] OSI SAF, Product Requirements Document, version 3.7, 07/11/2016t
SAF/OSI/CDOP2/M-F/MGT/PL/2-001

[AD.2] EUMETSAT, MTG End-User Requirements Document [EURD], version v3C, 30/03/2010
EUM/MTG/SPE/07/0036,

1.5. Scientific background

The radiative fluxes over ocean are mainly used as input to numerical ocean models or to biological studies (chlorophyll blooms, aquaculture). The accuracy requirements on the hourly MTG radiative fluxes [AD.1] are the same as those on MSG products: a 10% bias and 30% standard-deviation for the solar flux and a 5% bias and 10% standard-deviation for the longwave flux, the percentages being relative to the mean value and the statistics being on a monthly period.

Radiative flux retrievals from satellite data has begun in the 1980s, processing various satellites and instruments. The retrieval methods can be separated into two types: parameterizations (Tarpley, 1979, Gautier et al., 1980, Darnell et al., 1992) and Radiative Transfer Model (RTM) calculations (Schmetz, 1989; Pinker and Laszlo, 1992; Hollman et al.,2006).

The OSI SAF SSI algorithm is a physical parameterization applied to a visible channel (METEOSAT or GOES-E radiometer), after Gautier et al. 1980 and Frouin and Chertock, 1992. The LSA SAF follows the same method as OSI SAF, but using three SEVIRI channels instead of one and an actual surface albedo (Geiger et al. 2008) and the CM SAF follows a RTM approach (Hollman et al.,2006).

The OSI SAF DLI algorithm is a bulk parameterization using air temperature and humidity predicted by a NWP model and cloud information derived from satellite data. Bulk parameterizations are commonly used for air-sea interface studies based on meteorological observations, while satellite methods are often based on RTM calculations. The LSA SAF follows a bulk parameterization and the CM SAF a RTM approach.

The OSI, CM and LSA SAF radiative fluxes have been compared and validated against in situ measurements, over Europe (Ineichen et al., 2009) and over Africa (Ineichen, 2010), with a focus on SSI as the pyrgeometer measurements were too few. The two studies conclude that the products from the different SAFs have comparable biases and precisions, showing that the OSI SAF parameterizations compare favourably with the more complex RTM methods. So the OSI SAF algorithms used for MSG are maintained for MTG.

1.6. Characteristics of MTG/FCI

The Flexible Combined Imager (FCI) performs radiometric measurements in sixteen channels: five in the visible region of the spectrum, three in the near infrared and eight in the infrared (table 1). The spatial resolution at the satellite sub-point is 1 km for visible and near infrared channels and 2 km for infrared channels. The full disk is scanned with a basic repeat cycle of 10 minutes [AD.2]

CHANNEL	CENTRE WAVELENGTH	SPECTRAL WIDTH	SPATIAL SAMPLING DISTANCE (SSD)
VIS 0.4	0.444 µm	0.060 µm	1.0 km
VIS 0.5	0.510 µm	0.040 µm	1.0 km
VIS 0.6	0.640 µm	0.050 µm	1.0 km; 0.5 km*
VIS 0.8	0.865 µm	0.050 µm	1.0 km
VIS 0.9	0.914 µm	0.020 µm	1.0 km
NIR 1.3	1.380 µm	0.030 µm	1.0 km
NIR 1.6	1.610 µm	0.050 µm	1.0 km
NIR 2.2	2.250 µm	0.050 µm	1.0 km; 0.5 km*
IR 3.8 (TIR)	3.800 µm	0.400 µm	2.0 km; 1.0 km*
WV 6.3	6.300 µm	1.000 µm	2.0 km
WV 7.3	7.350 µm	0.500 µm	2.0 km
IR 8.7 (TIR)	8.700 µm	0.400 µm	2.0 km
IR 9.7 (O_3)	9.660 µm	0.300 µm	2.0 km
IR 10.5 (TIR)	10.500 µm	0.700 µm	2.0 km; 1.0 km*
IR 12.3 (TIR)	12.300 µm	0.500 µm	2.0 km
IR 13.3 (CO_2)	13.300 µm	0.600 µm	2.0 km

Table 1 : characteristics of the FCI instrument

2. SSI algorithm

The OSI SAF physical parameterization is applied separately to every pixel of a satellite image. The various steps of the method are presented below.

2.1. Calibration

The satellite visible count, VIS 0.6 of CFI, is converted into a bi-directional reflectance. The formulation of equation (1) depends on the instrument. The formula recommended by EUMETSAT for CFI will be applied.

$$L_{sc} = L_{sc}(t, C) \quad (1)$$

$$R_{nb} = L_{sc} / (\nu(j)\, \mu_0) \quad (2)$$

$$\nu(j) = 1 + 0.0334 \cos[2\pi\,(j-2) / 365.25] \quad (3)$$

with

L_{sc} : scaled radiance i.e. radiance divided by the solar spectral irradiance convoluted with the radiometer filter

R_{nb} : narrowband reflectance (relative to the band of the radiometer spectral filter)

C : radiometer count

t : current time (julian day)

$\mu_0 = \cos(\theta_0)$ θ_0 being the sun zenith angle

$\nu(j)$: corrective term accounting for the Earth-sun distance seasonal variation, j is the day of year

2.2. Narrow to broadband conversion

The reflectance relative to the narrow band of the radiometer spectral filter is converted into the reflectance relative to the broadband of the solar spectrum. As proposed in Pinker and Lazlo, 1992, this conversion is made with a linear formula :

$$R = M\, R_{nb} + B \quad (4)$$

where the M and B coefficients depend on the scene type. Instead of one type “cloud” as in Pinker and Lazlo, 1992, several types of clouds have been introduced, since the reflectances of fractional and semi-transparent clouds vary with the underlying surface.

The coefficients used for SEVIRI 0.6 μm visible channel are based on the well-calibrated broadband radiometer CERES (Clouds and Earth’s Radiant Energy System). They have been obtained by regression on METEOSAT-8/SEVIRI and CERES co-located data, supplied by Nicolas Clerbaux. The SEVIRI coefficients will be used for CFI 0.6 μm visible channel.

	cloud over ocean	cloud over vegetation	cloud over desert
M	0.819	0.774	0.814
B	0.023	0.063	0.030

***Table 2*: narrow to broadband band coefficients for the 0.6 μm visible channel of SEVIRI.

All pixels are considered as cloudy in the narrow to broadband band conversion. This short cut is possible because the visible channel data are ignored for clear pixels (see 2.4).

2.3. Anisotropy correction

The broadband bi-directional reflectance is converted into the Top Of Atmosphere (TOA) albedo, which is independent of satellite viewing angle. This step is based on the Manalo-Smith et al. 1998 formulas (derived from Earth Radiation Budget Instrument data), where the anisotropic factor is an analytical function of the viewing angles depending on the scene type.

$$A(\theta_0) = R / f_{aniso} \qquad (5)$$

with

- A : TOA albedo
- R : broadband reflectance
- f_{aniso} : anisotropic factor or bi-directional reflectance function (BDRF)

2.4. SSI parameterization

2.4.1. TOA albedo to SSI

The SSI parameterization separates clear sky and cloudy sky cases, which are identified by the cloud classification of the Nowcasting (NWC) SAF [RD.1]. The equations, after Gautier et al, 1980, are the following:

if clear $$E = E_0 \, \nu(j) \, \mu_0 \, T_a \qquad (6)$$

if cloudy $$E = E_0 \, \nu(j) \, \mu_0 \, T_1 \, T_{cl} \qquad (7)$$

$$T_{cl} = T_c / (1 - T_{bc} A_s . A_c) \qquad (8)$$

$$T_c = 1 - A_c - A_c \, m \, \mu_0 \qquad (9)$$

$$A = A_{ray} + T_{2top} A_c + A_s T_2 T_c^2 / (1 - T_{bc} A_s . A_c) \qquad (10)$$

with

- E : surface solar irradiance
- E_0 : solar constant
- T_a : clear sky atmospheric transmittance (sun-surface with multiple scattering)
- T_1 : sun-surface atmospheric transmittance, without multiple scattering
- T_2 : sun-surface-satellite transmittance
- T_{2top} : sun-cloud-satellite transmittance
- T_{bc} : transmittance below cloud, a constant value of 0.96 is assumed
- A_{ray} : Rayleigh albedo
- A_s : surface albedo
- A_c : cloud albedo
- T_c : cloud transmittance
- T_{cl} : cloud factor
- m : cloud absorption factor

For a clear pixel, equation (6), the TOA solar irradiance is attenuated by the clear sky atmospheric transmittance. The TOA albedo is not used, the satellite data are used only through the cloud classification.

For a cloudy pixel, the SSI is derived from the TOA albedo through equations (7) to (10). Equation (7) express the SSI as the TOA solar irradiance attenuated by an atmospheric transmittance and a cloud factor, which depends on the cloud transmittance and cloud albedo (equation (8)). Equation (9) relates the cloud transmittance and the cloud albedo, assuming that the cloud absorption linearly depends on the cloud albedo with a constant coefficient m. The TOA albedo, equation (10), is the sum of three terms: Rayleigh scattering, radiation reflected by cloud and attenuated by the atmosphere and radiation reflected by the surface and attenuated by the atmosphere and the cloud. As the TOA albedo is known, solving equations (9) and (10) allows to calculate the cloud albedo and the cloud transmittance. The SSI is then calculated by equations (8) and (7).

2.4.2. Surface albedo

The sea surface albedo is calculated theoretically, while the land surface albedo is derived from an atlas. They vary with respect to the sun zenith angle, after Briegleb et al., 1986 formulas.

land $A_s = A_s(0)\ (1+2d) / (1+2d\ \mu_0)$ $d = 0.4$ (11)

sea with clear sky : $A_s = 0.026/(0.065+ \mu_0^{1.7}) + 15.0\ (\mu_0-0.1)\ (\mu_0-0.5)\ (\mu_0-1.)$ (12)

sea with cloudy sky : $A_s = 0.06$ (13)

2.4.3. Amospheric transmittances

All atmospheric transmittances are obtained by analytical formulas, depending on viewing angles, atmospheric parameters.

The sun-surface atmospheric transmittance, T_a and T_1, are calculated after Frouin and Chertock, 1992, by the following equations :

$$T_1 = e^{-\tau_{h2o}}\ e^{-\tau_{o3}}\ e^{-\tau_{sc}} \quad (14)$$

$$T_a = T_1 / [\ 1 - A_s\ (\ a' + b'/ V)\ ] \quad (15)$$

$$\tau_{h2o} = 0.102\ (W / \mu_0)^{0.29} \quad (16)$$

$$\tau_{o3} = 0.041\ (\ U_{o3} / \mu_0\ )^{0.57} \quad (17)$$

$$\tau_{sc} = (a + b / V) / \mu_0 \quad (18)$$

with

W total water vapor content of the atmosphere in $g.cm^{-2}$

U_{o3} total ozone content of the atmosphere in cm atm

V horizontal visibility in km

a, b, a', b' : coefficients depending on the aerosol type

maritime :	a = 0.059	b = 0.359	a' = 0.089	b' = 0.503
continental :	a = 0.066	b = 0.704	a' = 0.088	b' = 0.456

Equation (18) accounts for multiple scattering between surface and cloud, using a climatological aerosol background.

The double path atmospheric transmittances, T_2 and T_{2top}, differ only by the water vapor absorption, the wator vapor content above cloud is assumed to be 30% of the total content. The ozone and water vapor absorption and the Rayleigh scattering formulas are from Lacis and Hansen, 1974 .

$$T_2 = 1 - a_{o3}(U_{o3}\ M) - a_{h2o}(W\ M) - A_{ray}(\mu_0) - A'_{ray}(\mu) \quad (19)$$

$$T_{2top} = 1 - a_{o3}(U_{o3}\ M) - a_{h2o}(0.3\ W\ M) - A_{ray}(\mu_0) - A'_{ray}(\mu) \quad (20)$$

$$a_{h2o}(x) = 2.9\ x / (1. + 141.5\ x)^{0.635} + 5.925\ x \quad (21)$$

$$a_{o3}(x) = a_{o3}^{VIS}(x) + a_{o3}^{UV}(x) \quad (22a)$$

$$a_{o3}^{VIS}(x) = 0.02118\ x / (1. + 0.042\ x + 0.000323\ x^2) \quad (22b)$$

$$a_{o3}^{UV}(x) = 1.082\ x / (1. + 138.6\ x)^{0.805} + 0.0658\ x / [1 + (103.6\ x)^3] \quad (22c)$$

$$A_{ray}(\mu_0) = 0.28 / (1 + 6.43\ \mu_0) \quad (23)$$

$$A'_{ray}(\mu) = 0.0685. \quad (24)$$

where

$M = (1 / \mu_0 + 1 / \mu)$

$\mu = \cos(\theta)$ θ being the satellite zenith angle

The formulations of the single path and double path transmittances differ, as a result from a study on a matchup data set gathering GOES-E data and pyranometer measurements (Brisson et al., 1999). On clear sky cases, better SSI results were obtained with Frouin and Chertock, 1992 formulas (equations (14)-(18)). On cloudy cases, the calculated minimun and maximum albedos agree better with observed satellite values, when using Lacis and Hansen, 1974 formulas (equations (19)-(24)).

The cloud absorption factor, m in equation (9), has been tuned on actual satellite data. The tuned value is not fully independent of the radiometer calibration, however the values obtained in several experiments were rather close (Le Borgne et al., 2005). The OSI SAF operational chain has used 0.15 as of March 2005, for GOES-E and MSG imagers. This value will be used for CFI.

2.4.4. Sun glint algorithm

The preliminary step is to identify the pixels affected by sunglint. This step is done with the method used in the NWC cloud classification scheme. In case of sunglint, the clear sky SSI is calculated with equation (6) and a specific scheme is applied to the cloudy pixels.

The bi-directional reflectance $R_{PCocean}$ of the type "partly cloudy over ocean" (Manalo-Smith et al. 1998 formulas) and the cloud type are used to identify the pixels affected by an important sunglint. For these pixels, the cloud albedo A_c is not calculated with equations (9)-(10) but assumed, otherwise the usual algorithm, equations (7)-(10), is used. The cloudy pixels processing can be summarized as follows:

if (fractional cloud or thin cirrus) and ($R_{PCocean} > 0.2$)

$A_c = 0.2$

SSI is calculated with equations (7)- (9)

else

SSI is calculated with equations (7)- (10)

This empirical approach has been verified by the fact that, in the present OSI SAF chain, an hourly SSI field does not show artefacts in the sunglint area, which is obvious in the corresponding visible image.

3. DLI algorithm description

The OSI SAF DLI algorithm is a bulk parameterization combining NWP model outputs and satellite derived cloud parameters, which are cloud types derived from the NWC SAF classification [RD.1] for nighttime pixels and clear to cloudy SSI ratio for daytime pixels. The formulas are presented below.

$$L = (\varepsilon_0 + (1 - \varepsilon_0)\, C)\, \sigma\, T_a^4 \qquad (25)$$

$$\varepsilon_0 = 1-(1+\xi)\exp\{-(1.2 + 3.0\,\xi)^{1/2}\} \; -0.05\,(p_0-p) / (p_0-710) \qquad (26)$$

$$\xi = 46.5\,(e / T_a) \qquad (27)$$

if day $\quad C = 1 - E / E_{clear} \qquad (28)$

if night $\quad C = C_i \qquad (29)$

with

L	: downward longwave irradiance at the Earth's surface (W/m^2)	
ε_0	: clear sky emissivity	
C	: infrared cloud amount	
T_a:	: near surface air temperature (K)	
σ	: Stefan-Boltzmann constant	$\sigma = 5.6696\ 10^{-8}$ W m^{-2} K^{-4}
e	: near surface surface water vapor pressure (hPa)	
p	: surface atmospheric pressure (hPa)	
p_0	: normal atmospheric pressure, 1013.25 hPa	
E	: surface solar irradiance (W/m^2)	
E_{clear}	: clear sky surface solar irradiance (W/m^2)	
C_i	: contribution coefficient of this cloud type	

The DLI is calculated as the sum of a clear sky and cloudy sky contributions (equation (25)). The clear sky emissivity is derived from the near surface air temperature and water vapor pressure (equations (26) and (27)), according to the formulation proposed by Prata, 1996. The infrared cloud amount, which gives the cloudy sky contribution, is obtained by two different formulations:

- For daytime cases, equation (28), the infrared cloud amount is deduced from the actual to clear sky SSI ratio, as proposed by Crawford and Duchon, 1999.
- For nighttime cases, equation (29), the infrared cloud amount is the cloud contribution coefficient of the cloud type covering the pixel.

The DLI cloud types correspond to a simplified cloud classification, merging several types of the NWC SAF detailed cloud classification [RD.1]. The values of the cloud contribution coefficients, presented in table 3, have been adjusted on a 1-year data base (July 97 to June 98) gathering DLI measurements, GOES-8 data and observed air temperature and humidity (Brisson et al., 2000). The NWC SAF detailed cloud types have evolved since 1998 but they have always been merged into the same simplified cloud types. These simplified cloud types will be used for MTG/CFI.

DLI cloud type	C_i	DLI cloud type	C_i
clear	0	fractional cloud	0.15
low cloud	0.82	volcanic ash	0
medium cloud	0.78	sand cloud	0.52
high opaque cloud	0.72	unclassified	0
thin cirrus	0.11	clear re-classified	0
thick cirrus	0.49	medium dubious	0.15

Table 3 **:** cloud types and cloud contribution coefficients (C_i).

4. Radiative flux processing overview

4.1. Products

The delivered MTG products are the continuation of the MSG products, i.e. hourly products on a 0.05 grid [AD.1].There are several types of radiative flux products, all in netcdf4 format:

1) fluxes in satellite space view at full resolution, not delivered to users:
   - fluxes directly calculated from FDC data — so-called SAT
   - fluxes interpolated at rounded UT hours — so-called PRD
   - daily fluxes — so-called DAY

2) fluxes re-mapped onto a regular grid, delivered to users:
   - fluxes interpolated at rounded UT hours
   - daily fluxes

   Characteristics of the grid:
   Projection: linear scaling in latitude and longitude
   Resolution: 0.05 degree in latitude and longitude
   Coverage: 60S - 60N; 60 W - 60E

4.2. Hourly calculations

A radiative flux product calculated on the original satellite data is not homogeneous in time. The pixel time varies from north to south, depending on the satellite (less than 10 minutes for MTG with the basic repeat cycle, about 12 minutes for MSG data and about 24 minutes for GOES-E data). This temporal variation cannot be neglected for the SSI, which directly depends on the sun zenith angle. The OSI SAF has chosen to calculate products interpolated at rounded UT hours, which are more user friendly and fully consistent between two different satellites.

First, the radiative fluxes are calculated with the algorithms presented in sections 2 and 3, on FDC data at nominal times (H – 10 minutes) and H, H being a UT rounded hour. They are stored in workfiles, which contain, in particular, the cloud albedo obtained with the SSI and the cloud contribution obtained with the DLI.

Then, the radiative fluxes are calculated at H, pixel by pixel. All time dependant parameters (viewing angles, surface albedo, atmospheric absorption) are calculated at H. The cloud albedo and the cloud contribution are interpolated between the values available before and after H, which allows to calculate the SSI and the DLI, respectively.

The interpolation scheme can cope with eventual missing images and produces a value in any case, decreasing the quality level (see 4.4):

- if only one value is available, instead of the before-and-after values, this value is used as of,
- eventually, a default value is used: 0.22 for the cloud albedo and 0.29 for the cloud contribution

4.3. Daily calculation

The daily value is the mean irradiance over a UT day. As the PRD products do not have missing values, the daily DLI is simply the mean of all hourly values in the UT day. The SSI daily integration is slightly more complicate, since it accounts for the sunrise and sun set times, calculated independently for every pixel. The solar day may be fully included in the UT day or corresponds to two uncompleted solar days: day 1 / night / day 2. This configuration is observed with GOES-E data but not with MTG data.

4.4. Quality levels

Similarly to the SST products, each pixel DLI or SSI value, is associated to a quality level expressed on a scale showing 6 values : 0 : unprocessed, 1 : erroneous , 2: bad, 3: acceptable, 4: good, 5 : excellent. The quality level values will follow the same rules as those of the present MSG operational chain (presented below). Some minor changes are possible, to account for MTG processing scheme characteristics.

The 0 value corresponds most of the time to space, the 1 value corresponds to an error in the software logic and should not occur. The other value meanings depend on the products and are described below.

<u>SSI SAT</u>

5: nominal calculation

4: SSI calculation with a minor problem:

sunglint

TOA albedo too low, case considered as clear

TOA albedo too high, maximum cloudiness assumed, SSI=0

<u>DLI SAT</u>

5: DLI value calculated with the daytime method (SSI ratio)

4: DLI value calculated with the nighttime method (NWC classification)

Values 3 and 2 are unused for the SAT products.

<u>SSI or DLI PRD</u>

The PRD flux value is interpolated between SAT values, as explained in 4.3; its quality level is obtained as follows:

5: interpolation between two SAT values both having a quality level of 5

4: interpolation between two SAT values with quality levels (4,5) or (4,4)
3: interpolation with only one SAT value: sunrise, sunset or missing value
2: no SAT value available, using default cloud albedo or contribution

SSI or DLI DAY

The quality level is the rounded mean of the PRD quality levels associated to the fluxes entering into the daily integration; this produces a value from 2 to 5.

4.5. Ancillary and auxiliary data

All data needed for the processing of the radiative fluxes are listed in tables 4 and 5. The data are separated in so-called auxiliary data, which are static (atlas and climatology) and ancillary data, which are dynamic (NWP forecast and satellite products). Except for aerosols, the tables describe the status in MSG operational chain

parameter	Source	Use
Air temperature and humidity at 2m, surface pressure	ECMWF NWP forecast	clear sky DLI
Air temperature and humidity profiles	ECMWF NWP forecast	calculate total water vapor content for SSI transmittances
Cloud types	NWC SAF cloud classification	SSI calculation DLI cloud contribution
Aerosols	TBD	SSI and DLI validation

Table 4*:* ancillary data

Parameter	Source	Use
Land-sea atlas	World Vector Shoreline	identify land and sea pixels (SSI)
Mean altitude	global atlas GTOPO30	calculate total water vapor content for SSI transmittances
Surface type	CERES land cover type atlas	NB to BB conversion (SSI)
Surface albedo	monthly climatology Csiszar and Gutman, 1999	SSI calculation over land
Specific humidity profiles	Ort monthly climatology	calculate total water vapor content for SSI transmittances
Ozone	TOMS monthly climatology	SSI transmittances
Visibility	latitude and month tabulated Stuhlman et al, 1990	SSI transmittances

Table 5 : auxiliary data

All ancillary and auxiliary data are first remapped onto the space view grid and then temporally interpolated at the product time.

The integrated water vapour content is derived from the NWP air temperature and humidity profiles and from the altitude atlas. The specific humidity climatology is used only if the NWP atmospheric profiles are missing.

4.6. Remapping

The OSI SAF distributed products are obtained by remapping at the nearest neighbour the PRD and DAY products onto a regular 0.05° grid. The remapping is a final step, which simply re-distributes the radiative fluxes and quality level values without changing them.

5. Possible changes in the methods

The MTG processing baseline, described in sections 2 to 5, is based on the present MSG operational chain, with the same algorithms and processing scheme. If specific studies are done before MTG operations showing improved SSI results, some changes are possible, such as:

- using several CFI channels instead of one in order to obtain the broadband reflectance,
- changing the transmittance parameterization for better results at low latitudes,
- updating the auxiliary data,
- replacing the climatological surface albedos by actual values.

6. Continuous control and validation plan

It is assumed that OSI SAF will process both a MTG satellite and a GOES-E satellite, as in the present operational chain.

6.1. Control

The aim of a continuous control is to make available on a near real time basis (immediately after the production of radiative fluxes) relevant information to detect quickly a problem in the functioning of the chain The control is performed outside the operational environment. It consists in a series of quicklooks, statistics and graphics (partly visible to external users), which are listed below:

- quicklooks of the hourly and daily DLI and SSI products,
- quicklooks of quality levels for a subset of products,
- statistics of (GOES-E – MTG) difference in the overlapping area are daily calculated . The hourly and daily DLI and SSI statistics are plotted as a function of time (figure 1).

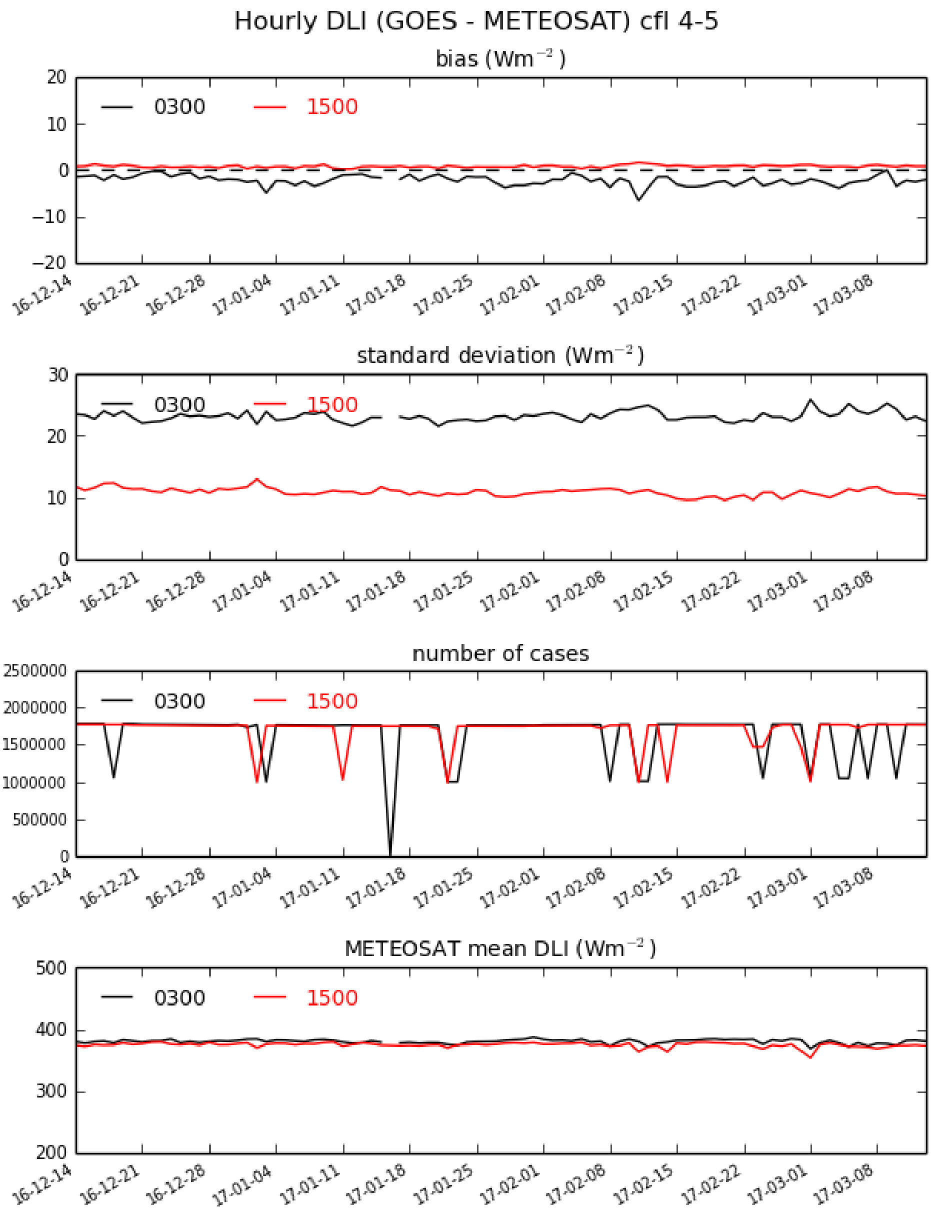

Figure 1: hourly DLI differences, GOES-E minus METEOSAT, at 00:00 UT and 15:00 UT

6.2. Validation plan

Similarly to the present MSG operational chain, the validation of MTG chain is based on Match-up Data Sets (MDS) gathering coincident MTG data and in situ measurements, from pyranometer (SSI) or pyrgeometer (DLI).

Before the processing chain becomes operational, a study will be done in order to check that the requirements are fulfilled. A report will be produced, similar to to the validation report [RD.2], associated to an upgrade of GOES-E and MSG chain.

The operational validation will be done a monthly basis, because some station networks deliver their data at this frequency.

6.2.1. The Matchup data set

MDS files are built routinely for the SAT, PRD and DAY products over a current set of stations, coming from several networks. The satellite data are ingested in near real time and the in situ measurements with a longer delay (one month to several years). Fixed or mobile stations can be added offline into the MDSs, in order to process easily data from oceanographic campaigns.

The measured flux in the MDS is a value centered on the time of the satellite data, obtained from the original in situ data by integration or interpolation. The calculated flux and its quality index are stored on a square box centered on the measurement station. Two options are prepared for the satellite versus in situ comparison in the SAT and PRD MDS:

a. the calculated flux averaged over the box versus the measured flux integrated over 1 hour.

b. the calculated flux at the central pixel of the box versus the measured flux integrated over 10 minutes

Option a has been used for all OSI SAF radiative flux products, option b is more natural from a user point of view (Ineichen et al., 2009).

Tthe SAT MDS files contains rcomplementary dat, such as the parameters used in the processing and meteorological measurements at the station. The Saharan Dust Index (SDI), which is not present in the MSG MDS, will be included in the MTG MDS.

6.2.2. Statistics

The operational validation is done as follows:

- on a monthly basis, which is the delivering frequency of some measuring networks
- MTG and GOES -E results are merged, due to the limited number of stations,
- two sets of stations (one for SSI and one for DLI) are defined, gathering stations rather well distributed in the area and delivering their measurements in a reasonable delay (figure 2).

Basic statistics of the SSI or DLI difference (calculated minus measured) are computed for all products (SAT, PRD, DAY), per station and for sets of stations.

Graphics , relative to the SSI and DLI operational sets of stations, are produced:

- scatterograms of calculated flux vs measured flux,
- monthly mean and standard deviation of the flux difference, in percentage of the mean measure (figure 3),
- mean and standard deviation of the flux difference as a function of time (figure 4),
- mean and standard deviation of the flux difference per station (figure 5).

Most of the graphics are visible to the users.

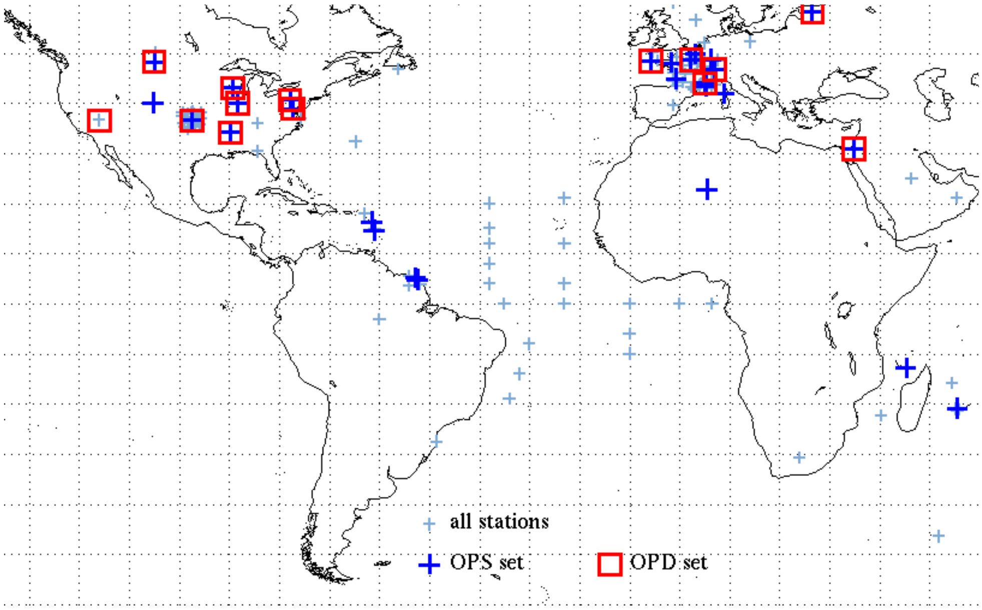

Figure 2 :map of the pyranometer and pyrgeometer stations used in 2017, OPS is the operational set for SSI validation, OPD the operational set for DLI validation

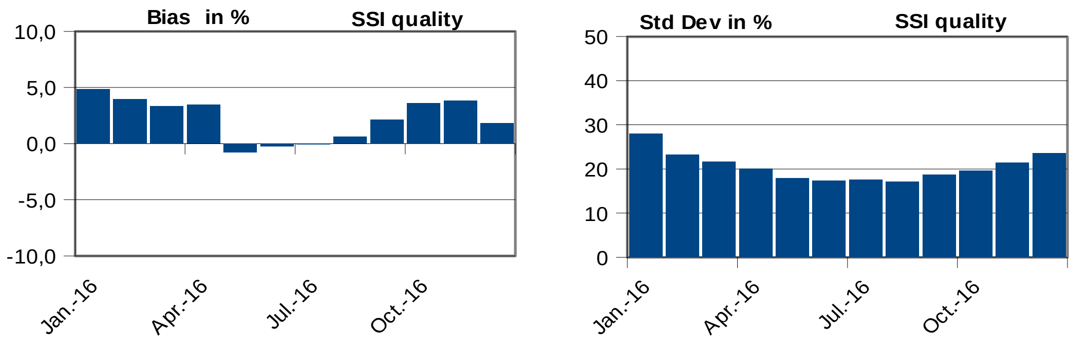

F

Figure 3: hourly SSI monthly statistics over 1 year, in percentage of the mean measure, from [RD.3]. The left plot shows the mean of the SSI difference and the right plot shows the standard deviation.

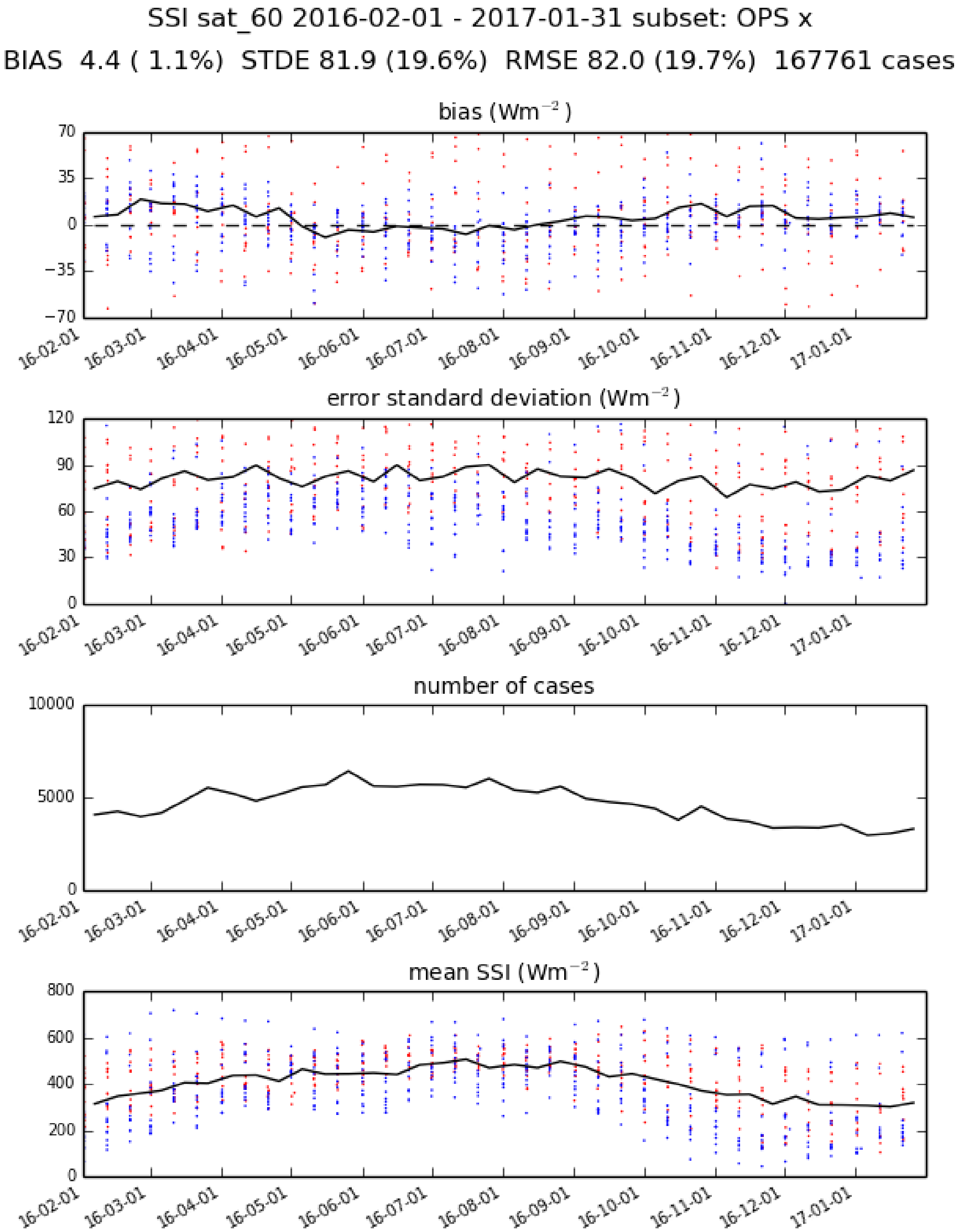

Figure 4 : hourly SSI validation statistics one 1-year period

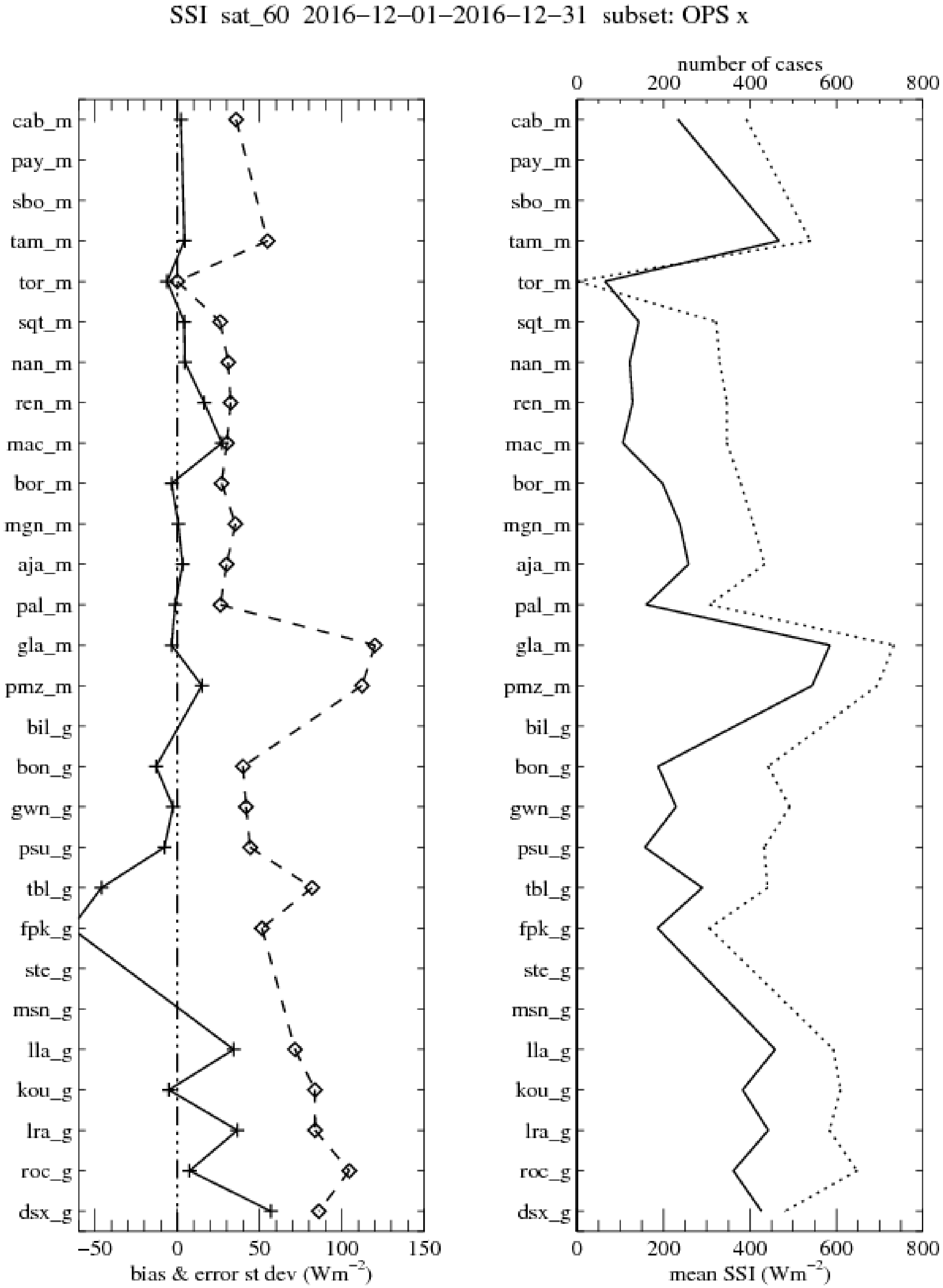

Figure 5: hourly SSI validation statistics per station in December 2016., left plot showing mean (solid) and standard deviation (dashed) of the SSI difference and right plot mean SSI (solid) and number of cases (dotted).

7. References

Briegleb B. P., P. Minnis, V. Ramanathan and E. Harrison, 1986, Comparison on regional clear-sky albedos inferred from satellite observations and model computations, Journal of Climate and Applied Meteorology, 25, 214-226.

Brisson, A., P. LeBorgne, A. Marsouin, 1999, Development of algorithms for Surface Solar Irradiance retrieval at OSI SAF low and Mid Latitude, February 1999. Météo-France/DP/Centre de Météorologie Spatiale, BP 147, 22302 Lannion, France.

Brisson, A., P. LeBorgne, A. Marsouin, 2000, Development of algorithms for Downward Long wave Irradiance retrieval at O&SI SAF Low and Mid Latitudes, O&SI SAF Report to EUMETSAT.

Crawford T.M. and C.E. Duchon, 1999, An improved parameterization for estimating effective atmospheric emissivity for use in calculating daytime downwelling longwave radiation. Journal of Applied Meteorology, 38, 474-480.

Csiszar I. and G. Gutman, 1999, Mapping global land surface albedo from NOAA AVHRR, JGR vol. 104, D6, 6215-6228

Darnell W.L. Staylor, W.F., Gupta, S.K., Ritchey, N.A. and Wilbur, A. C., 1992, Seasonal variation of surface radiation budget derived from international satellite cloud climatology project C1 data, Journal of Geophysical Research, 97, 15,741-15,760.

Frouin R. and B. Chertock, 1992, A technique for global monitoring of net solar irradiance at the ocean surface. Part 1: Model, Journal of Applied Meteorology, 31,1056-1066.

Gautier C, Diak G, Masse S. 1980. A simple physical model to estimate incident solar radiation at the surface from GOES satellite data. Journal of Climate and Applied Meteorology. 19: 1005-1012

Geiger B, C. Meurey C, D. Lajas, L. Franchistéguy, D. Carrer D,and JL Roujean ,2008, Near real-time provision of downwelling shortwave radiation estimates derived fromsatellite observations. Meteorological Applications, 15, pp. 411–420.

Gupta, S.K., W.K. Darnell and A.C. Wilber, 1992, A parameterisation for longwave surface radiation from satellite data: recent improvements. Journal of Applied Meteorology, 31,pp. 1361–1367.

Hollmann R, Mueller RW, Gratzki A. 2006. CM-SAF surface radiation budget: First results with AVHRR data. Advances in Space Research. 37: 2166-2172.

Ineichen P. , C.S. Barroso, B. Geiger, R. Hollmann, A. Marsouin and R. Mueller, 2009, Satellite Application Facilities irradiance products: hourly time step comparison and validation over Europe, IJRS, Vol. 30, No. 21, November 2009, 5549-5571

Ineichen P 2010,. *Satellite based short wave irradiance validation over Africa*., Visiting scintist report;

Lacis AA, Hansen JE. 1974. A parameterization for the absorption of solar radiation in the Earth's atmosphere. Journal of the Atmospheric Sciences. 31: 118-133.

Manalo-Smith N., G.L. Smith, S. N. Tiwari and W.F. Staylor, 1998, Analytic forms of bidirectional reflectance functions for application to Earth radiation budget studies, Journal of Geophysical Research, Vol. 103, D16, pp. 19,733-19,751, August 27, 1998.

Pinker, R.T., and Laszlo, I., 1992, Modeling surface solar irradiance for satellite applications on global scale, Journal of Applied Meteorology, 31, 194-211.

Prata, A.J., 1996, A new long-wave formula for estimating downward clear-sky radiation at the surface, Quarterly Journal of the Royal Meteorological Society, 122, 1127-1151.

Stuhlmann, R., M. Rieland and E. Raschke, 1990, An improvement of the IGMK Model to derive total and diffuse solar radiation at the surface from satellite data, Journal of Applied Meteorology 29, 586-603.

Tarpley JD. 1979. Estimating Incident Solar Radiation at the Surface from Geostationary Satellite Data. Journal of Applied Meteorology. 18: 1172-1181.